

# Development of a New Infrared Device for Monitoring the Coefficient of Variation in Yarns

Chang-Chiun Huang, Tsann-Tay Tang

Department of Polymer Engineering, National Taiwan University of Science and Technology, Taipei, Taiwan

Received 7 December 2005; accepted 17 August 2006

DOI 10.1002/app.25441

Published online 26 July 2007 in Wiley InterScience (www.interscience.wiley.com).

**ABSTRACT:** The coefficient of variation (CV) in yarns is the most important evenness characteristic in textile processing and quality control. This article develops a new infrared device for monitoring the coefficient of variation in yarns, based on on-line measurement of the yarn diameter, during the yarn manufacturing process. The device is composed of a 555 astable oscillator, four pairs of infrared emitters and receivers, a summing amplifier, an inverting amplifier, an alternating current (AC) to direct current (DC) converter, a unity-gain second-order Sallen–Key low-pass filter, and a data acquisition system. The optimum values of some factors with the circuit, including the oscillator frequency, amplified gain, cutoff frequency of the

low-pass filter, sampling time, and number of sampling data to be averaged in the moving average method, are systematically chosen by the Taguchi method to reduce the variance in the output voltage of the device. The CV based on measured yarn diameter data is transformed to that based on mass profiles. The experimental results reveal that the CVs evaluated by the infrared device are close to those by the Uster Evenness Tester, which is verified by the statistical analysis of variance. © 2007 Wiley Periodicals, Inc. *J Appl Polym Sci* 106: 2342–2349, 2007

**Key words:** coefficient of variation; infrared device; Taguchi method

## INTRODUCTION

The coefficient of variation (CV), defined as the mass variation per unit length or the diameter variation of yarns, has been the most important evenness characteristic in textile processing and quality control.<sup>1</sup> The yarn irregularity often makes yarns tend to break in spinning, weaving, and knitting, and causes periodic faults with fabrics in finishing and dyeing. Moreover, the appearance, hairiness, strength, and productivity of yarns are critically influenced by the yarn CV, which directly affects the cost and quality of a product. Hence, monitoring the yarn CV is one of the important ways to enhance product quality. Currently, the Uster Evenness Tester has been widely used to measure the yarn CV; however, it is not suitable for on-line measurement in a yarn-manufacturing environment, because it is sensitive to both temperature and humidity. Therefore, we develop a new infrared device to evaluate the yarn CV as precisely as the Uster Evenness Tester, and it is able to work on-line during yarn production processes. The device also has merits of low cost and a common way of signal transmission to a computer. Any environmental disturbance and circuit noise will deteriorate measurement accuracy of the device.

We use the systematic Taguchi method in circuit design so as to reduce the effect of the disturbance and noise on the measurement.

In the past years, the yarn CV has been measured by pressure rollers, air flow, radiation, photoelectric elements, capacity, microwave, and image processing. Tsai and Chu<sup>2</sup> developed a new photoelectric sensor that measured the yarn diameter and yarn CV on-line. The data acquisition system consisted of a 12-bit A/D converter, a 8255 I/O board, and industrial microcomputer based on a 80486-25 processor. The yarn CV was calculated by the measured yarn diameter and the area-compensation method. The experimental results showed that the mean of ten CVs is 17.8% for the inhomogeneous radiant flux and 15.4% for the homogeneous radiant flux with a 13.9-tex ring-spun yarn, compared with 14.3% for the Uster Evenness Tester. The photoelectric sensor could work when the yarn moved and vibrated, and was immune from the influence of temperature and humidity. However, the light emitting diode (LED) with the sensor, directly driven by a higher current, had a shorter life, and the sensor was sensitive to environmental light. Sparavigna et al.<sup>3</sup> revealed that the yarn CV was evaluated with an optical measuring system, sensitive to the light absorbed and diffused by a moving yarn. The system was composed of two light emitting diodes, two charge coupled device (CCD) cameras, two amplifiers, and the digital acquisition system connected to a computer with a RS232. The thickness of the yarn was converted into

Correspondence to: C.-C. Huang (huangcc@mail.ntust.edu.tw).

a proportional electrical voltage called a yarn signal by the optical system, and the CV was calculated based on the yarn signal. Although the optical sensor was suitable for on-line measurement of yarn CVs, it was subject to environmental constraints, high cost, and long computation time. In melt spinning, on-line measurements of fiber diameters have been developed by the existing commercial measurement devices. Kikutani et al.<sup>4</sup> developed a diameter measurement system by three diameter monitors, enabling us to measure the movement of diameter profiles based on the back-illumination principle. The monitors provided a noncontact technique for accurate measurement of diameters within 2 mm in the spinline velocity of 10,000 m/min. Nevertheless, the cross-sectional shape of as-spun fiber was noncircular, and the on-line measurement of fiber thickness by a single direction might not be the true diameter. Rovere et al.<sup>5-7</sup> presented that the fiber diameter was measured on-line by taking high speed flash photography and viewing the negatives under a Nikon microscope with a micrometer eyepiece. To provide an accurate reference standard, a fine wire of known diameter was photographed simultaneously with the spinline. The camera and flash were mounted on a traverse system that permitted measurements at many positions along the spinline. However, the measured fiber diameters were often higher than off-line measurements due to burred edges of fibers.<sup>8</sup>

This article develops an infrared device to monitor the yarn CV based on on-line measurement of the yarn diameter, which can work in a yarn-manufacturing environment. The device involves the 555 astable oscillator, summing amplifier, inverting amplifier, alternating current (AC) to direct current (DC) converter, unity-gain Sallen–Key low-pass filter, and data acquisition system. For extending the life and reducing the cost of the device, the device uses an astable oscillator to trigger the infrared LED and applies the serial communication to send the signal to a computer. Since the serial communication easily causes transmitted noise, we adopt the moving average method to reduce the noise. To alleviate the effects of environment disturbances and circuit noises on the output voltage, we systematically select the optimum values of some factors with the device circuit by the Taguchi method.<sup>9</sup> The factors include the oscillated frequency, amplified gain, cutoff frequency, sampling time, and number of sampling data to be averaged in the moving average method. An emitter light directs to a yarn and its receiver senses the yarn shadow. The device finally outputs the yarn diameter in a voltage signal. The diameter data are used to calculate the CV and the CV is then transformed to that based on the yarn mass. The results are compared with those by the Uster Evenness Tester.

## THEORY

### Unity-gain second-order Sallen–Key low-pass filter<sup>10,11</sup>

A second-order filter is generally characterized by the filter type, gain, center frequency, and filter quality factor. For an ideal low-pass filter, it completely eliminates signals above the cutoff frequency, and perfectly passes signals below the cutoff frequency. Changing the gain or center frequency alters the amplitude or frequency scale on an amplitude response curve, but the shape remains the same. The quality factor determines the relative shape of the amplitude response. The general second-order low-pass filter has the transfer function of the form

$$H(s) = \frac{H_0}{\frac{1}{\omega_0^2} S^2 + \frac{1}{Q\omega_0} s + 1} \quad (1)$$

where  $H_0$  is the gain,  $\omega_0$  is the center frequency in radian, and  $Q$  is the quality factor. The filter has the best gain accuracy because its gain is independent of component values. Its architecture is shown in the block of the low-pass filter of Figure 1. At points a and b, the current equations with parameter  $s$  by the Kirchoff's law are written as

$$\frac{V_a - V_{11}}{R_{29}} = \frac{V_b - V_a}{\frac{1}{sC_6}} + \frac{V_b - V_a}{R_{30}} \quad (2)$$

$$\frac{V_b - V_a}{R_{30}} = \frac{-V_b}{\frac{1}{sC_5}} \quad (3)$$

where  $V_b = V_{12}$ . By combining eqs. (2) and (3), we get the transfer function as follows:

$$H(s) = \frac{V_{12}}{V_{11}} = \frac{1}{C_5 C_6 R_{29} R_{30} s^2 + C_5 (R_{29} + R_{30}) s + 1} \quad (4)$$

Comparing eqs. (1) and (4), we obtain  $H_0 = 1$ ,  $1/\omega_0^2 = C_5 C_6 R_{29} R_{30}$ , and  $1/Q\omega_0 = C_5 (R_{29} + R_{30})$ . Since  $\omega_0 = 2\pi f_c$ , where  $f_c$  is the cutoff frequency of the low-pass filter in Hertz, the cutoff frequency and quality factor in the filter are given by

$$f_c = \frac{1}{2\pi \sqrt{R_{29} R_{30} C_5 C_6}} \quad (5)$$

$$Q = \frac{\sqrt{R_{29} R_{30} C_5 C_6}}{C_5 (R_{29} + R_{30})} \quad (6)$$

### Taguchi experiment design<sup>12</sup>

To deal with complex design of experiments in a simple way, the Taguchi method adopts systematically a

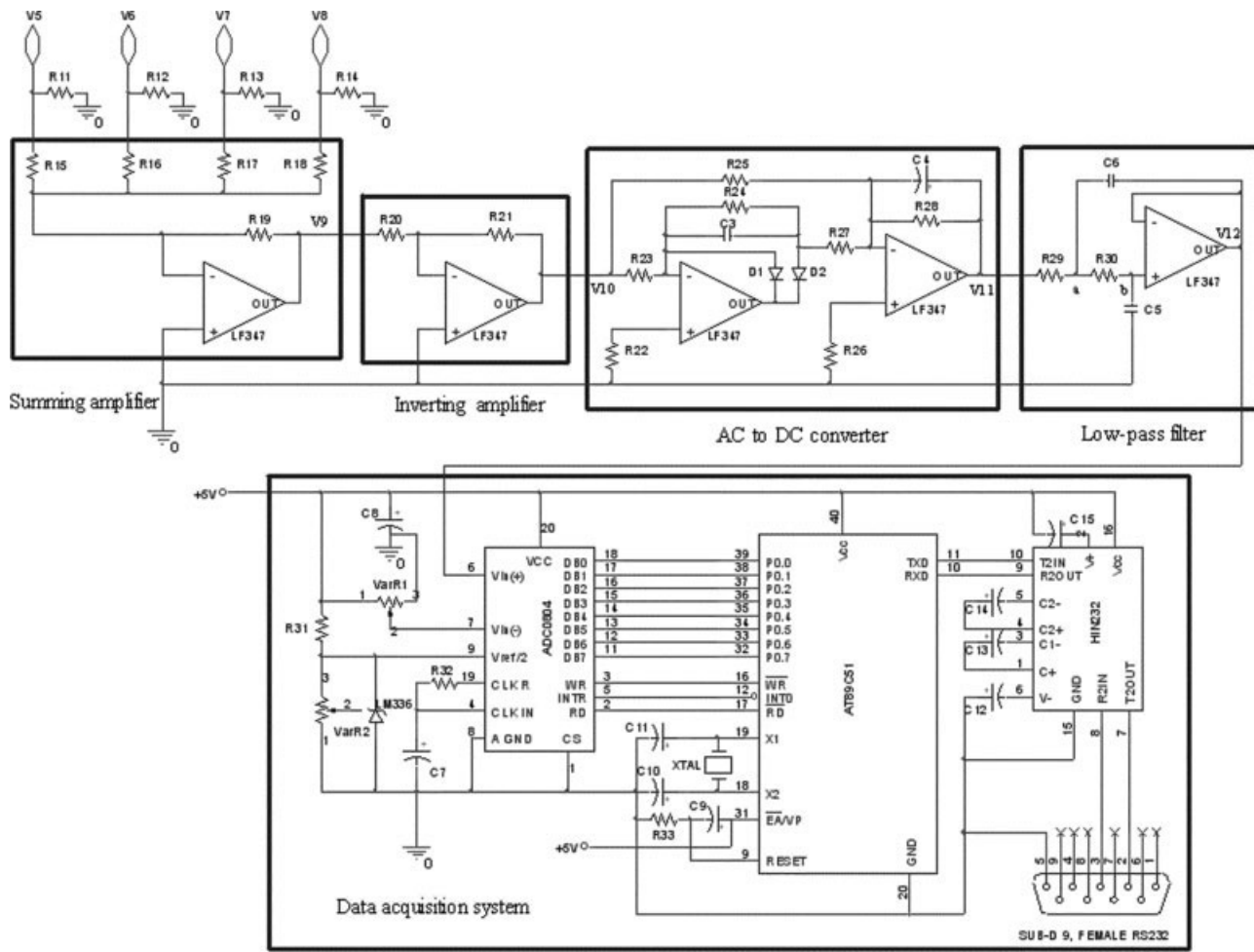


Figure 1 Circuit layout of the infrared device.

special design of the orthogonal array (OA) to study the entire parameter space with a small number of experiments. The OA is a matrix arranged in columns and rows. Each column represents a control factor. Meanwhile, each row represents the state of the control factor. Each experiment trial is carried out based on its factor-level combination in each row. Since the variance in the output voltage of the device is to be minimized, the smaller-the-better characteristic is used for the quality analysis as follows:

$$SN = -10 \times \log_{10} \left( \frac{1}{n} \sum_{i=1}^n y_i^2 \right) \quad (7)$$

where  $n$  denotes the number of repetition data in each trial and  $y_i$  represents the  $i$ th measured quantity. The larger SN ratio indicates the better quantity characteristics.

The means of SN ratios at the same level for all control factors are computed to give the response table. The optimum factor-level combination is selected based on the highest response values in the response

table. Moreover, the predicted SN ratio  $\hat{\eta}$  at the optimum factor-level combination can be calculated as

$$\hat{\eta} = \eta_m + \sum_{i=1}^p (\bar{\eta}_i - \eta_m) \quad (8)$$

where  $\bar{\eta}_i$  denotes the mean response,  $\eta_m$  represents the mean of total SN ratios, and  $p$  is the number of significant factors identified via the analysis of variance (ANOVA) and  $F$ -test.

Finally, a confirmation experiment is performed to verify the reproducibility of the experiment, based on the confidence interval (CI) by Eq. (9). Once the error between the predicted and experimental SN ratio is within the interval of  $-CI$  and  $CI$ , the experiment is demonstrated to be reproducible.

$$CI = \sqrt{F_{\alpha,1,v_2} \times V_e \times \left[ \left( 1 + \sum_{i=1}^p \text{dof}_i / N_d \right) + 1/r \right]} \quad (9)$$

where  $F_{\alpha,1,F_2}$  represents  $F$ -ratio,  $\alpha$  denotes the risk,  $v_2$  is the number of degrees of freedom associated with the

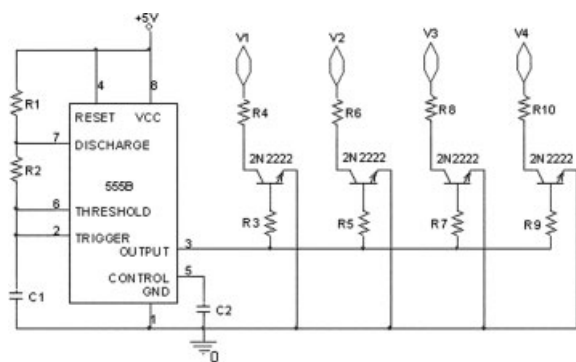


Figure 2 555 Astable oscillator.

pooled error variance ( $V_e$ ) of the experiment,  $N_d$  represents the trial number of OA,  $dof_i$  is the degrees of freedom associated with significantly factors, and  $r$  is the sample size for the confirmation experiment,  $r \neq 0$ .

**Coefficient of variation<sup>13</sup>**

In handling large quantities of data statistically, the CV is commonly used to define their variability and is thus well-suited to the problem of expressing yarn evenness. Currently, it is probably the most widely accepted way to quantify irregularity. The yarn CV based on the diameter data is given by the following expression:

$$CV_d = \frac{\sqrt{V_d}}{\bar{d}} \tag{10}$$

where  $\bar{d} = \frac{1}{n} \sum_{i=1}^n d_i$  is the mean of yarn diameter data and  $V_d = \sum_{i=1}^n (d_i - \bar{d})^2 / (n - 1)$  is the variance.

We can transform the yarn CV based on measured diameter profiles to that based on mass profiles. The

relationship is constructed based on a geometrical and statistical model to evaluate the effects of the measuring field length. We assume that the geometrical shape of a yarn cross section is circular and the density of a yarn is uniform along the yarn length. The expectation of yarn mass can be expressed in terms of the diameter statistics as follows:

$$\bar{m} = \frac{\rho\pi}{4} \{V_d + \bar{d}^2\} \tag{11}$$

where  $\rho$  is the density of a yarn. Under the assumption that the diameter values of a yarn are normally, independently, and identically distributed, the variance of mass can be expressed as

$$V_m = \left(\frac{\rho\pi}{4}\right)^2 \{4\bar{d}^2 V_d + 2V_d^2\} \tag{12}$$

The yarn CV based on mass profiles, defined as  $CV = \sqrt{V_m/\bar{m}}$ , and modified by a coefficient of 1/2, is given by

$$CV = \frac{1}{2} \frac{CV_d \sqrt{4 + 2CV_d^2}}{1 + CV_d^2} \tag{13}$$

**EXPERIMENTAL RESULTS**

The infrared device is composed of the 555 astable oscillator, summing amplifier, inverting amplifier, AC to DC converter, unity-gain Sallen–Key low-pass filter, and data acquisition system, whose circuit layouts are shown in Figures 1 and 2. The infrared device generally suffers from the environment disturbances, the noise of circuits, the distortion of sampling signals, and the noise of serial communication.

TABLE I  
L<sub>16</sub> Orthogonal Array and SN Ratios

| Trial no. | A                          | B              | C                     | D                  | E              | SN ratios |
|-----------|----------------------------|----------------|-----------------------|--------------------|----------------|-----------|
|           | Oscillated frequency (kHz) | Amplified gain | Cutoff frequency (Hz) | Sampling time (ms) | Average number |           |
| 1         | 1                          | 1              | 1                     | 1                  | 1              | 24.44     |
| 2         | 1                          | 2              | 2                     | 2                  | 2              | 27.32     |
| 3         | 1                          | 3              | 3                     | 3                  | 3              | 12.19     |
| 4         | 1                          | 4              | 4                     | 4                  | 4              | 23.64     |
| 5         | 2                          | 1              | 2                     | 3                  | 4              | 14.28     |
| 6         | 2                          | 2              | 1                     | 4                  | 3              | 22.29     |
| 7         | 2                          | 3              | 4                     | 1                  | 2              | 11.37     |
| 8         | 2                          | 4              | 3                     | 2                  | 1              | 22.67     |
| 9         | 3                          | 1              | 3                     | 4                  | 2              | 18.19     |
| 10        | 3                          | 2              | 4                     | 3                  | 1              | 16.96     |
| 11        | 3                          | 3              | 1                     | 2                  | 4              | 25.71     |
| 12        | 3                          | 4              | 2                     | 1                  | 3              | 26.03     |
| 13        | 4                          | 1              | 4                     | 2                  | 3              | 15.72     |
| 14        | 4                          | 2              | 3                     | 1                  | 4              | 26.68     |
| 15        | 4                          | 3              | 2                     | 4                  | 1              | 9.67      |
| 16        | 4                          | 4              | 1                     | 3                  | 2              | 16.06     |



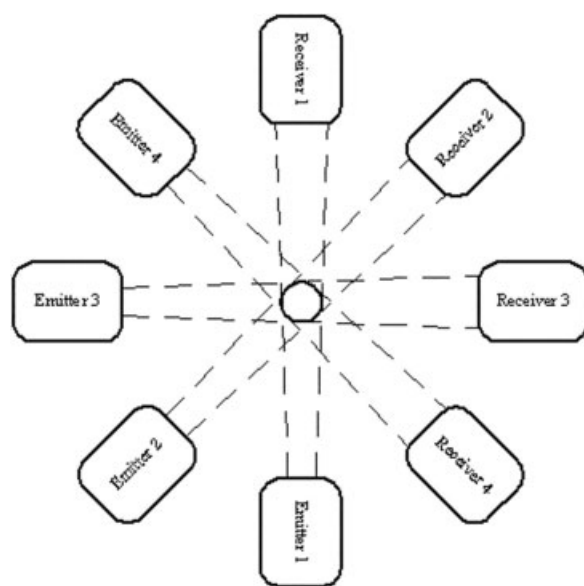


Figure 3 Placement of four pairs of emitters and receivers.

To alleviate the effects of the disturbances and noises on the device, we attempt to choose the optimum values of factors, which include the oscillated frequency (Factor *A*), amplified gain (Factor *B*), cutoff frequency (Factor *C*), sampling time (Factor *D*), and number of sampling data to be averaged in the moving average method (Factor *E*), to reduce the variance in the output voltage of the device. Factors *A* and *C* are the frequencies in Hertz. Factor *D* is the time in milliseconds. Since a four-level factor has three degrees of freedom, five four-level factors require fifteen degrees of freedom. In general, the experimenter should seek the smallest OA, which has at least fifteen degrees of freedom. Here, an  $L_{16}$  OA with five columns and sixteen rows as shown in Table I is used. This array has fifteen degrees of freedom and can handle five four-level factors. Thus, only sixteen experiment trials are required to study the entire parameter space.

The 555 astable oscillator is used to generate a square wave at a desired frequency. The square wave is fed into a transistor that drives an infrared LED emitter on and off very rapidly. The frequency  $f$  in Hertz is calculated by  $f = 1/C_1(R_1 + 2R_2) \ln 2$ , and the duty-cycle  $D$  is computed by  $D = R_2/(R_1 + 2R_2)$ .<sup>14</sup>

TABLE II  
Level Values of Factors

| Level | <i>A</i> | <i>B</i> | <i>C</i> | <i>D</i> | <i>E</i> |
|-------|----------|----------|----------|----------|----------|
| 1     | 4        | 1        | 25       | 20       | 10       |
| 2     | 8        | 2        | 50       | 10       | 20       |
| 3     | 12       | 4        | 100      | 5        | 30       |
| 4     | 16       | 6        | 150      | 1        | 40       |

TABLE III  
Response Table

| Level | <i>A</i>           | <i>B</i>           | <i>C</i>           | <i>D</i>           | <i>E</i>           |
|-------|--------------------|--------------------|--------------------|--------------------|--------------------|
| 1     | 21.90 <sup>a</sup> | 18.16              | 22.13 <sup>a</sup> | 22.13              | 18.44              |
| 2     | 17.65              | 23.31 <sup>a</sup> | 19.33              | 22.86 <sup>a</sup> | 18.23              |
| 3     | 21.72              | 14.73              | 19.93              | 14.87              | 19.06              |
| 4     | 17.03              | 22.10              | 16.92              | 18.45              | 22.58 <sup>a</sup> |

<sup>a</sup> Denotes the highest value of each factor among the four levels.

The duty-cycle generally cannot overstep 50%; otherwise the 555 integrated circuit (IC) will be damaged immediately. Thus, with the selection of  $C_1 = 0.1 \mu\text{F}$  and  $R_1 = 270 \Omega$ , we set the oscillator frequencies at 4, 8, 12, and 16 kHz for four-level values to give the resistor  $R_2$  of 1645, 767, 463, and 314  $\Omega$ , respectively.

The infrared LED receivers have been triggered off by oscillated signals that are close to emitter frequencies. When an emitter light directs to a yarn, its receiver senses the yarn shadow and outputs a voltage signal. Since the cross section of a yarn may not be circular, we place four pairs of emitters and receivers, each having an angle span of  $45^\circ$  with another one, around a circle with the yarn passing through the center as shown in Figure 3. Thus, the yarn diameters viewed from four angles are measured in signals  $V_5$ ,  $V_6$ ,  $V_7$ , and  $V_8$ . The four signals merge and flow through the resistor  $R_{19}$  in the summing amplifier. If the resistors  $R_{15}$ ,  $R_{16}$ ,  $R_{17}$ , and  $R_{18}$  are equal to  $R$ , the signal  $V_9$  is proportional to the sum of the four signals as  $V_9 = -R_{19}/R(V_5 + V_6 + V_7 + V_8)$ ,<sup>15</sup> where the amplified gain is  $R_{19}/R$ . With  $R = 10 \text{ k}\Omega$ , we set the four-level values of the amplified gain at 1, 2, 4, and 6 by selecting  $R_{19}$  of 10, 20, 40, and 60 k $\Omega$ , respectively. The summing amplifier is then connected to the inverting amplifier, which is the unity gain because the resistor  $R_{20}$  is equal to the resistor  $R_{21}$ , for transforming the signal  $V_9$  to the inphase receiver signal  $V_{10}$ . We convert the signal  $V_{10}$  into a pure DC signal  $V_{11}$  by an AC to DC converter,<sup>16</sup> which involves a half wave rectifier and feed-forward compensation. The compensation sums the half wave rectified signal and the signal  $V_{10}$  to provide a full wave signal. The time constant must be much greater than the maximum period of the signal  $V_{10}$  for reducing the gain error at

TABLE IV  
Analysis of Variance

| Factor     | SS     | dof | <i>V</i> | <i>F</i> |
|------------|--------|-----|----------|----------|
| <i>A</i>   | 80.77  | 3   | –        |          |
| <i>B</i>   | 183.17 | 3   | 61.06    | 2.97     |
| <i>C</i>   | 54.91  | 3   | –        |          |
| <i>D</i>   | 162.71 | 3   | 54.24    | 2.64     |
| <i>E</i>   | 49.54  | 3   | –        |          |
| Pool error | 185.22 | 9   | 20.58    |          |
| Total      | 531.1  | 15  |          |          |

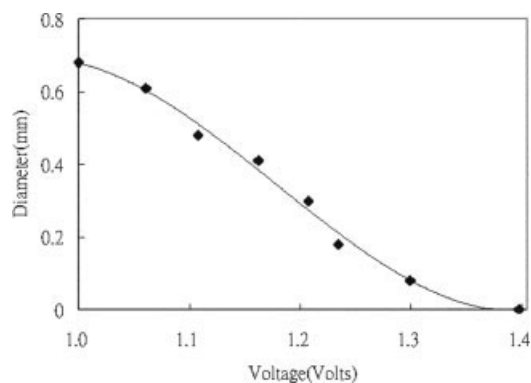


**Figure 4** Relationship between voltage and yarn diameter.

high frequencies. The time constant,  $R_{28}C_4$ , is about 0.2 s by choosing  $R_{28} = 22.2 \text{ k}\Omega$  and  $C_4 = 10 \text{ }\mu\text{F}$ . The signal  $V_{11}$  is calculated by  $V_{11} = R_{28}V_{10}\left[\frac{1}{R_{27}} - \frac{1}{R_{25}}\right]$  with  $R_{25} = 20$  and  $R_{27} = 10 \text{ k}\Omega$ .

The output signal of the infrared device is small, allowing it to be partially obscured by the noise of the device and its amplifier. If the cutoff frequency of a low-pass filter is high enough to allow the desired frequencies of signals to pass, the overall noise level can be reduced. The unity-gain Sallen–Key low-pass topology<sup>17</sup> is shown in Figure 1, where the quality factor  $Q$  is usually lower than 3. The capacitors  $C_5 = C_6 = 0.1 \text{ }\mu\text{F}$ , the resistor  $R_{29} = 10 \text{ k}\Omega$ , and the resistor  $R_{30}$  of 400, 100, 25, and 11.6 k $\Omega$  give the four-level values of 25, 50, 100, and 150 Hz, respectively, for the cutoff frequencies by Eq. (5); thus the low-pass filter has the quality factor  $Q$  of 0.15, 0.29, 0.45, and 0.50, respectively, by Eq. (6).

The data acquisition system uses an ADC0804 chip to convert the analog signal  $V_{12}$  into the digital signal. We connect pin CS of the chip to the ground so that the ADC0804 chip is always enabled.<sup>18</sup> The

$V_{12}$  is limited to a voltage between 0 and 5 V by setting the reference voltage of 2.5 V and connecting pin  $V_{in(-)}$  to the ground. The signal  $V_{12}$  is converted into the digital signal whose decimal value is calculated by  $5V_{12}/255$ . Furthermore, an AT89C051 microcontroller connects the ADC0804 to the Hin232 chip, and controls the analog to digital conversion. The Hin232 accepts the standard digital logic value between 0 and 5 V and converts it to the RS232 standard of +10 and –10 V based on four capacitors  $C_{12}$ ,  $C_{13}$ ,  $C_{14}$ , and  $C_{15}$  of 22 pF. The data acquisition system will send a stream of values to the computer.

The four-level values of five factors are listed in Table II. We choose the quality characteristic of the standard deviation in the output voltage of the device, which is transformed into the SN ratio defined by the smaller-the-better characteristic as in Eq. (7). The number of repetition data is 10. The SN ratios for sixteen experiment trials are shown in the last column of Table I. The mean of SN ratios for the oscillated frequency (Factor A) at level 1 can be calculated by averaging the SN ratios for Trials 1–4. The mean of SN ratios for each level of the other factors can be computed in a similar manner. These mean values are summarized in the response table as displayed in Table III. The optimum factor-levels are selected by the highest response values marked by “\*” in the subscript, which are A1, B2, C1, D2, and E4. A1, B2, C1, D2, and E4 represent the oscillated frequency at Level 1, amplified gain at Level 2, cutoff frequency at Level 1, sampling time at Level 2, and number of sampling data to be averaged at Level 4, respectively.

ANOVA is performed by the SN ratios and calculated  $F$ -ratios with each factor. The contribution of factors with significantly lower variation than other factors can be pooled to estimate the total variation in the experiment. The pooled factors are indicated

**TABLE V**  
CV Comparison Between the Infrared Device and Uster Evenness Tester

| No.      | Cotton              |           |           | Polyester (115d/36f) |           |           | Polyester (230d/48f) |           |           |
|----------|---------------------|-----------|-----------|----------------------|-----------|-----------|----------------------|-----------|-----------|
|          | Infrared device (%) | Uster (%) | Error (%) | Infrared device (%)  | Uster (%) | Error (%) | Infrared device (%)  | Uster (%) | Error (%) |
| 1        | 21.29               | 21.67     | 1.74      | 16.96                | 16.89     | –0.41     | 17.15                | 17.51     | 2.08      |
| 2        | 21.41               | 20.98     | –2.04     | 17.52                | 17.08     | –2.58     | 16.78                | 17.70     | 5.19      |
| 3        | 21.09               | 22.01     | 4.20      | 17.19                | 16.98     | –1.23     | 17.79                | 17.79     | 0.02      |
| 4        | 21.74               | 21.32     | –1.96     | 16.49                | 16.50     | 0.05      | 17.45                | 17.59     | 0.79      |
| 5        | 21.93               | 21.35     | –2.70     | 17.01                | 16.94     | –0.43     | 17.08                | 16.95     | –0.78     |
| 6        | 21.17               | 22.08     | 4.12      | 17.01                | 17.46     | 2.60      | 17.80                | 17.53     | –1.55     |
| 7        | 20.65               | 21.50     | 3.96      | 17.27                | 17.44     | 0.98      | 17.24                | 16.65     | –3.54     |
| 8        | 21.18               | 21.99     | 3.70      | 17.24                | 17.59     | 1.99      | 16.90                | 17.57     | 3.79      |
| 9        | 20.78               | 21.56     | 3.61      | 17.63                | 17.58     | –0.29     | 17.51                | 17.46     | –0.31     |
| 10       | 21.55               | 21.17     | –1.80     | 17.09                | 17.68     | 3.33      | 16.53                | 17.37     | 4.84      |
| Mean     | 21.28               | 21.56     | 1.30      | 17.14                | 17.21     | 0.41      | 17.22                | 17.41     | 1.09      |
| Variance | 0.158               | 0.140     |           | 0.100                | 0.152     |           | 0.177                | 0.123     |           |

TABLE VI  
Closeness Justification of CVs Obtained by the Infrared Device and Uster Evenness Tester

|                     | Cotton         |               | Polyester (115d/36f) |               | Polyester (230d/48f) |               |
|---------------------|----------------|---------------|----------------------|---------------|----------------------|---------------|
|                     | Between groups | Within groups | Between groups       | Within groups | Between groups       | Within groups |
| SS                  | 0.41           | 2.69          | 0.03                 | 2.27          | 0.18                 | 2.70          |
| dof                 | 1              | 18            | 1                    | 18            | 1                    | 18            |
| V                   | 0.41           | 0.15          | 0.03                 | 0.13          | 0.18                 | 0.15          |
| F                   | 2.72           |               | 0.21                 |               | 1.19                 |               |
| Critical value in F | 4.41           |               | 4.41                 |               | 4.41                 |               |

by symbol “–” in Table IV. The results show that significant factors, *B* and *D*, are those whose *F*-ratios are bigger than  $F_{0.12,3,9}$  at the risk of 0.12.

The confirmation experiment is of utmost importance in the design of an experiment. The estimated SN ratios of the standard deviation in the output voltage using these optimum settings can be computed by Eq. (8). When comparing predicted and experimental values, good agreement may be assured if the error between them is within the interval of  $-CI$  and  $CI$ . The  $CI$  is calculated to be 6.63 by Eq. (9), where  $\alpha = 0.12$ ,  $v_2 = 9$ ,  $F_{0.12,3,9} = 2.95$ ,  $N_d = 16$ , and  $r = 10$ . In this case, the experimental and predicted values are 30.26 and 26.59, respectively; as a result, the error is 3.67 within the interval of  $-6.63$  and  $6.63$ . Hence, the results show good reproducibility of experimental data.

Steel bars with diameters of 0.08, 0.18, 0.30, 0.41, 0.48, 0.61, and 0.68 mm were used to construct the relationship between the diameter and output voltage of the infrared device. The relationship, shown in Figure 4, is approximated by a polynomial  $y = 18.097x^3 - 63.709x^2 + 72.312x - 26.026$ , where  $y$  and  $x$  indicate the yarn diameter and voltage, respectively. The infrared device is installed at the front of the Uster Evenness Tester. The yarn passes the infrared device and the Uster Evenness Tester at a speed of 25 m/min and testing time of 4 min. Three kinds of yarns, cotton, polyester (115d/36f) and polyester (230d/48f), were used. In the infrared device, the yarn shadow thickness is measured in the voltage, which is amplified, and then the voltage is transformed to the yarn diameter based on their relationship. The yarn evenness is evaluated by the coefficient of variation, CV, defined by a ratio between the standard deviation and the mean of yarn diameter data as in Eq. (10). The CV is then transformed to the CV based on the mass per unit length by Eq. (13). The yarn CVs by the infrared device are compared with those by the Uster Evenness Tester as displayed in Table V using the same ten pieces of yarns. The relative errors in CVs between our device and Uster Evenness Tester are from  $-3.54$  to  $5.19\%$ . The mean and variance of ten CVs are also computed and listed in Table V. The relative errors in mean values between our device and Uster Evenness

Tester are below 1.30%. The closeness of yarn CVs obtained by our device and Uster Evenness Tester is verified by the one-way ANOVA, in which the sums of squares (SS), degrees of freedom (dof), variances (V), and *F* ratios (*F*) are computed in Table VI. When the tabled critical value in the *F* ratio at the risk of 0.05 is larger than the calculated *F* ratio, we accept null hypothesis that the infrared device and Uster Evenness Tester perform equally. That is, the yarn CVs obtained from our device are close to those from Uster Evenness Tester. Therefore, our device can evaluate the yarn CV as accurately as the Uster Evenness Tester, and unlike the Uster Evenness Tester, it can be installed in a yarn-manufacturing site to monitor the yarn CV.

## CONCLUSIONS

This article develops a new infrared device to evaluate the yarn CV based on on-line measurement of yarn diameter, and the device is immune from severe influence of temperature and humidity. A data acquisition system uses a serial communication port to collect the yarn shadow thickness in a voltage signal. The device circuit is designed by using the Taguchi method to systematically determine the optimum values of some factors so that the environment disturbances and inherent circuit noises have a reduced effect on the output voltage of the device. The experimental results demonstrate that for yarns of cotton, polyester (115d/36f) and polyester (230d/48f), good agreement in CVs between our device and Uster Evenness Tester is justified by ANOVA.

## References

1. Slater, K. *Text Prog* 1986, 14, 23.
2. Tsai, S. I.; Chu, W. C. *J Text Inst* 1996, 87, 484.
3. Sparavigna, A.; Broglia, E.; Lugli, S. *Mechatronics* 2004, 14, 1183.
4. Kikutani, T.; Nakao, K.; Takarada, W.; Ito, H. *Polym Eng Sci* 1999, 39, 2349.
5. Balsal, V.; Shambaugh, R. L. *Polym Eng Sci* 1996, 36, 2785.
6. Balsal, V.; Shambaugh, R. L. *Polym Eng Sci* 1998, 38, 1959.
7. Rovere, A. D.; Shambaugh, R. L. *Polym Eng Sci* 2001, 41, 1206.

8. Bansal, V.; Shambaugh, R. L. *Ind Eng Chem Res* 1998, 37, 1799.
9. Taguchi, G.; Tsai, S. C. *IEEE Trans Reliab* 1995, 44, 225.
10. Lacanette, K. A basic introduction to filters-active, passive, and switched-capacitors; National Semiconductor Corporation, Santa Clara, CA, April 1991; Application note 779.
11. Texas Instruments. Active filter design techniques; Texas Instruments, TX, 2001; Chapter 16, Literature Number SLOA088.
12. Ross, P. J. *Taguchi Techniques for Quality Engineering*, 2nd ed.; McGraw-Hill: New York, 1996.
13. Jasper, W.; Suh, M. W.; Woo, J. L.; Kim, J.; Lee, S. National Textile Center Annual Report, National Textile Center, Spring House, PA, 1997.
14. National Semiconductor Corporation. LM 555 Timer, National Semiconductor Corporation, Santa Clara, CA, 2000.
15. Sedra, S.; Brackett, P. O. *Filter Theory and Design: Active and Passive*; Matrix Publishers: Portland, OR, 1978.
16. National Semiconductor Corporation. Precision AC/DC Converters, National Semiconductor Corporation, Santa Clara, CA, 1969; LB-8.
17. Texas Instruments. Analysis of Sallen-Key Architecture, Texas Instruments, TX, 1999; Application Report.
18. National Semiconductor Corporation. ADC0801/ADC0802/ADC0803/ADC0804/ADC0805 8 Bit uP Compatible A/D Converters, National Semiconductor Corporation, Santa Clara, CA, 1999.